

TOPOLOGY AND GEOMETRY OF CAUSTICS IN RELATION WITH EXPERIMENTS

ALAIN JOETS

*Laboratoire de Physique des Solides
Université de Paris-Sud, bât. 510
91 405 Orsay cedex France
E-mail: joets@lps.u-psud.fr*

Abstract. Caustics of geometrical optics are understood as special types of Lagrangian singularities. In the compact case, they have remarkable *topological* properties, expressed in particular by the Chekanov relation. We show how this relation may be experimentally checked on an example of biperiodic caustics produced by the deflection of the light by a nematic liquid crystal layer. Moreover the physical laws may impose a *geometrical* constraint, when the system is invariant by some group of symmetries. We show, on the example of polyhedral caustics, how the two constraints force degenerate umbilics of integer index to appear and determine their spatial organization.

1. Introduction. Caustics of geometrical optics have strongly stimulated the study of singularities [34]. They are now understood as a special class of singularities, the so-called Lagrangian singularities [1]. One of the main results of the theory of Lagrangian singularities in the ordinary space R^3 is their classification into five stable *local* types: A_2 (folds), A_3 (cusps), A_4 (swallowtails), D_4^- (elliptic umbilics) and D_4^+ (hyperbolic umbilics) [2]. Experiments in geometrical optics [35] and in wave optics [5, 7, 8] are in total agreement with this classification.

However it was rapidly realized that the caustics of geometrical optics form themselves a special class of Lagrangian singularities. Because of the eiconal equation [9], a system of rays is always associated with a Hamiltonian of special type, that is to say, convex with respect to the momenta. This property characterizes the (Lagrangian) optical singularities [11]. Every general Lagrangian singularity has *locally* an optical model [14] and the list of stable optical singularities remains the same, given by the five generic Lagrangian singularities. However it is not true that *globally*, a configuration of Lagrangian singularities can be realized optically. For example, the “pancake” caustic [37] has no optical

1991 *Mathematics Subject Classification*: Primary 78A05; Secondary 32S50.

The paper is in final form and no version of it will be published elsewhere.

realization. More generally the topology of caustics of geometrical optics is constrained by a relation linking the Euler characteristic χ_Σ of the singular set Σ , assumed to be compact, and the number $\#D_4(-1/2)$ of umbilics of index $-1/2$ [11]. This relation, due to Chekanov, has important consequences on the caustic metamorphoses [3, 36]. It is incompatible with some Lagrangian metamorphoses, reducing their number from eleven to seven [11].

These new theoretical results on the global properties of caustics assume generally some compactness hypothesis. On the other hand the caustics produced by experiments often present borders and/or asymptotic branches which prevent one from using them as experimental tests. We present here the first experimental examples of compact caustics. The first example (biperiodic caustics produced by the deflection of a light beam through a nematic liquid crystal layer) is used to check the topological constraint expressed by the Chekanov relation. Conversely, in the second example (the “poly-astroids” generated by surfaces with polyhedral symmetry), we start from the topological constraint and we show how, in the presence of a group of symmetry, it determines the spatial organization of the umbilics.

2. Biperiodic caustics. The usual optical sources (lasers, etc.) form systems of rays of limited aperture (few degrees) and do not allow the creation of compact wave fronts. However, a simple way to bypass this difficulty is to produce (in a necessarily limited domain of the space) a *biperiodic* wave front W . Indeed a biperiodic surface is topologically equivalent to a torus, which is a compact surface.

Experimentally, we realize the biperiodic front W by sending a light beam of parallel rays (direction z) across a transparent layer ($0 < z < d$) deflecting biperiodically the beam. Nematic liquid crystals are very appropriate materials for this experiment. First, because of their high birefringence, they strongly interact with the light [13]. They are optically uniaxial and the optic axis is directed along the local orientation of the rod-shaped molecules. This direction is denoted by a unit vector \vec{n} , the “director”. The energy index n for the extraordinary rays (the only rays considered here) is a function of the angle β between the ray direction \vec{r} and the director \vec{n} through the relation $n = \sqrt{n_o^2 \cos^2 \beta + n_e^2 \sin^2 \beta}$, where n_o and n_e are respectively the ordinary and the extraordinary refractive index [20]. The ray trajectories obey the Fermat principle, expressed by minimizing of the optical path $\int n ds$ [23]. Second, when submitted to the action of external forces (electric field, thermal gradient, etc.), the nematic layer may reach a stable stationary state characterized by some periodicity of the director alignment. For some values of the parameters, the structure is biperiodic in the plane $\{x, y\}$ of the layer (see [18] for the details of the experiment). It is named the varicose structure [28]. In the varicose structure the director field is well approximated by the form $\vec{n} = (\cos \phi, 0, \sin \phi)$, where $\phi = [\phi_1 \sin(k_{1x}x + k_{1y}y) + \phi_2 \sin(k_{2x}x + k_{2y}y)] \sin z\pi/d$, with $\phi_1 \neq \phi_2$.

The caustic C produced by the deflection of the light by the varicose structure is found to consist of a real and of a virtual part. The real part, which is the envelope of the emerging rays, is located above the layer ($z > d$). The virtual part, which is the

envelope of the prolongation of the emerging rays is located below the layer ($z < d$). The main part of the caustic surface is confined near the layer of width $d \simeq 100\mu\text{m}$ and a microscope is needed to observe it. It is important to understand here that the image obtained by the microscope is the section of the caustic by the focal plane Π of the instrument. The height (coordinate z) of Π may be easily varied and we are able in this way to reconstruct, section by section, the whole caustic C . In Fig. 1 a section of the real part and a section of the virtual part of C are represented. Each image consists of the same motif (unit cell) repeated by translation. The biperiodicity of the image corresponds with that of the director field of the varicose structure. Although the caustic appears as composed of two distinct parts, i.e. the real and the virtual parts, it must be understood as a connected surface, since the real and virtual parts connect at infinity along a “line” which corresponds to the stationary rays of the congruence.

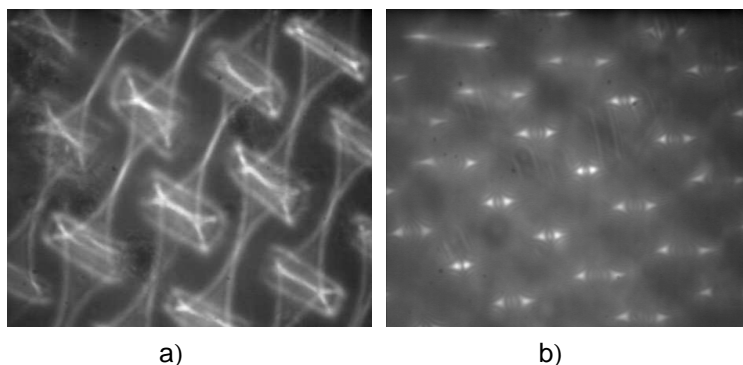


Figure 1: Two sections of the same biperiodic caustic produced by the deflection of a beam of parallel rays through a layer of nematic liquid crystal in convection (varicose structure). The focal plane of the microscope is located a) in the virtual part containing the hyperbolic umbilics, b) in the real part containing the elliptic umbilics.

The Chekanov formula states that the Euler characteristic χ_Σ of the singular Σ is related to the number $\#D_4(-1/2)$ of umbilics of index $-1/2$ by the relation $\chi + 2\#D_4(-1/2) = 0$ [11]. These umbilics correspond to the case II in the Darboux classification of umbilics [12]. They are named “Stars” in [6] and denoted by D_3 in [30]. They may be of elliptic type D_4^- or of hyperbolic type D_4^{+t} . In our case there exists an alternative form for the Chekanov relation. Since the rays are parametrized by the surface W and bear two caustic points, coinciding at the umbilics, the Euler characteristic χ_Σ is related to the Euler characteristic χ_W of W by the relation: $\chi_\Sigma = 2\chi_W - \#D_4$, where $\#D_4$ is the number of umbilics. Using this relation and the Chekanov relation, we recover the known fact that the total index I of the umbilics is equal to χ_W .

The initial wave front being equivalent to a torus, the expected value of the total index of the umbilics is 0, the Euler characteristic of the torus. Per unit cell, four (real) elliptic umbilics D_4^- and four (virtual) hyperbolic umbilics D_4^+ are observed (see Fig. 1). The index of the four D_4^- is $-1/2$ and they give a contribution to I equal to $4(-1/2) = -2$. The index of the D_4^+ may be *a priori* equal to $+1/2$ (umbilics D_4^{+d}) or to $-1/2$ (umbilics D_4^{+t}). It depends on the relative position of the singular set, of the kernel of the

Lagrangian projection, of the cusp-line passing through the umbilic and of the characteristic at the umbilic [11]. These elements lie in the phase space and they cannot be directly observed. They have to be found, for instance, by a numerical simulation. In our example the congruence of the rays is first calculated by numerical integration of the Euler-Lagrange equations associated with the minimization of the optical path and using the above expressions for the index n and for the director field \vec{n} . Then the Lagrangian projection is constructed and the different types of singularities are determined using their characterization by the rank [33, 19]. The result shows that the four hyperbolic umbilics are of type D_4^{+d} [21]. However there exists now a more practical way to determine directly the index in the real space [22]. First, let us distinguish two types of cusp points. A cusp point is said to be of type A_3^+ if the ray passing through the point is directed inward the cusp. It is said to be of type A_3^- in the opposite case. The type of the cusp lines changes at the umbilics. The index of a hyperbolic umbilic is equal to $+1/2$ if the ray passing through the umbilic, which is tangent to the cusp line at this point, is directed towards the A_3^- cusp line. It is equal to $-1/2$ if it is directed towards the A_3^+ cusp line. In our case the ray is directed towards the A_3^- cusp line and we recover immediately the result given by the simulation. The contribution of the D_4^+ (per unit cell) is then equal to $4(+1/2) = 2$, and the total index is 0, as expected. The Chekanov formula is experimentally checked. In this experiment, the Euler characteristic of the singular set Σ is found to be equal to -8 ($\chi_W = 0$, $\#D_4 = 8$). This value would disagree with that (zero) given in the reference [4, p. 97] for any compact Σ .

An interesting problem is to know if there exist other caustics with the same biperiodicity, but with a different number of umbilics (per unit cell). In particular it would be interesting to observe a caustic without any umbilic. This possibility seems to be theoretically allowed [26], but it has not been experimentally checked up to now.

3. “Poly-astroids”. Other interesting compact caustics are obtained when the wave front W is a nearly spherical surface. For instance, the Cayley astroid [10], which is the focal set of a triaxial ellipsoid, seems to provide the most simple example of such caustics, in the sense that the topological constraint $I = \chi_W$ is satisfied with a minimal number of generic umbilics.

From the experimental view point, as it was recalled in the previous section, it is difficult to produce a complete convex wave front. However there exists a formal analogy between this optical problem and other physical problems, for instance the problem of the stability of a magnetic nanoparticle placed in a magnetic field \vec{H} . There, the equilibrium conditions, expressing that the energy $E(\vec{m}; \vec{H})$ of the particle is minimal with respect to the orientation of its magnetization \vec{m} on the unit sphere, define convex level surfaces $W_{\text{mag}} = \{\vec{H}, E(\vec{H}) = \text{const.}\}$ [24, 31]. The magnetizations corresponding to the minima are normal to the surface W_{mag} (see Fig. 2). They play the role of the directions of the rays in the optical problem. The caustic of W_{mag} has a physical meaning. It represents the fields \vec{H} for which the magnetization orientation undergoes a jump (switching field). It may be experimentally determined, but only one sheet of the caustic surface may be observed [32].

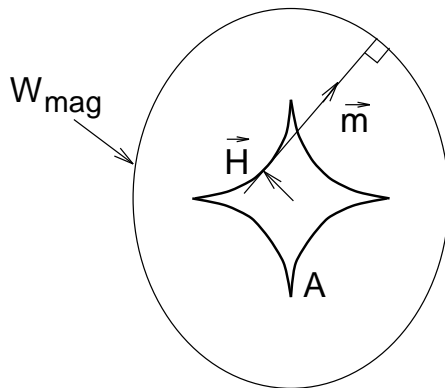


Figure 2: Sketch of the astroid A of the switching fields in the 2D case. For a given \vec{H} , the extrema of the energy E correspond to magnetizations \vec{m} tangent to A and normal to W_{mag} . When \vec{H} crosses A , a minimum \vec{m} (represented on the Figure) collides with another extremum (not represented) and one observes a jump in the direction of the magnetization.

The switching fields generally form an astroid, topologically equivalent to the Cayley astroid. However, for some values of the parameters of the problem, one finds a different type of astroid with degenerate umbilics [32]. For these particular values, the energy surface W and the associated caustic become symmetric, and the symmetry forces non-generic singularities to appear. More generally, a physical system may become symmetric for a continuous set of values of the parameters when the symmetry results from the physical laws, the boundary conditions or from some external fields. An example is provided by the stable biperiodic caustics of the previous section. A natural and important question is then to know what becomes a (compact) caustic in presence of a symmetry. Two constraints are now present: the topological constraint imposing that the total index I is equal to 2, the Euler characteristic of the sphere, and the geometrical constraint imposing that the singularities must be compatible with the symmetry. This difficult problem is here attacked on a particular example, in the case of a polyhedral symmetry. However we shall show that the solutions found are essentially determined by these two constraints.

To model a symmetrical wave front (or the energy surface of a nanoparticle) W we introduce n points P_i on the unit sphere and n masses m_i . We define the function V by

$$(1) \quad V(P) = \sum_{i=1}^n m_i d(P, P_i)$$

where $d(P, P_i)$ denotes the distance from P to P_i , and we assume that $m_i = 1/n > 0$ for all i , so that $V(0) = 1$. The surface W is taken as a level surface $W = \{P, V(P) = \text{const.}\}$. We impose the polyhedral symmetry by taking the P_i at the vertices of a regular polyhedron. Moreover we take $\text{const.} = 2$. The shape of the corresponding caustics surfaces is reproduced in Fig. 3 for the tetrahedron (Fig. 3a), the cube (Fig. 3b), the octahedron (Fig. 3c), and the dodecahedron (Fig. 3d). Each caustic is composed of two sheets which connect at the umbilic points. Each sheet is represented separately on Fig. 3 for a better understanding. We call them polyhedral caustics or “poly-astroids”. The caustic of

the icosahedron is not represented, because it is topologically equivalent to that of the dodecahedron. However this result does not mean that the symmetry itself determines the caustic, since two different poly-astroids are obtained in the cubic case (Fig. 3b and Fig. 3c).

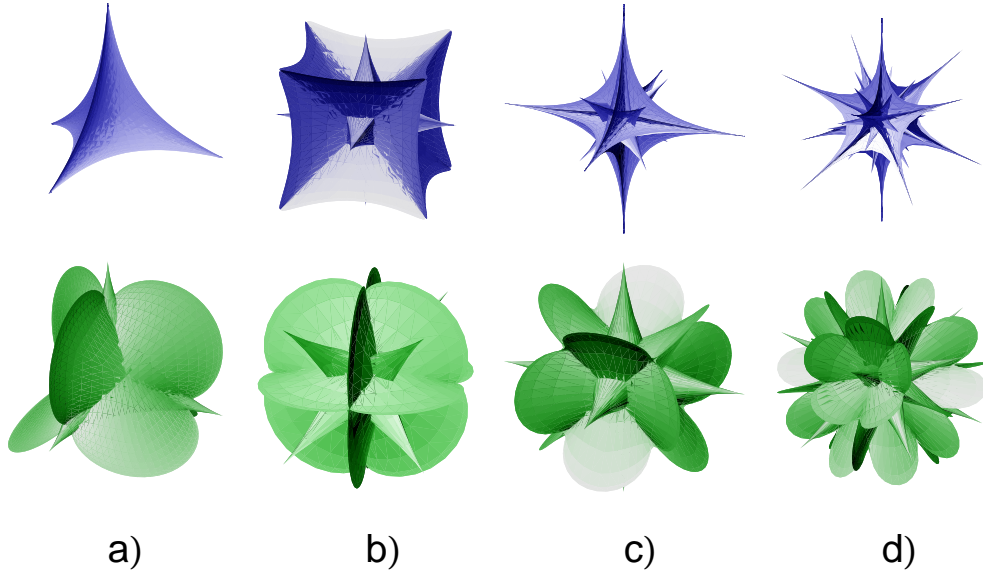


Figure 3: The elementary poly-astroids. They are obtained starting from a) a tetrahedron, b) a cube, c) an octahedron and d) a dodecahedron. Each caustic is composed of two sheets represented separately.

The caustic surfaces are very intricate, because of the presence of many self-intersection lines. We focus our attention on the singularities of smallest dimension, i.e. the point singularities. The complete description of the poly-astroids will appear in a forthcoming paper. The point singularities lie on the axes of symmetry of order 3, 4 and 5, and eventually on some mirror planes. For each polyhedron, the symmetry axes of order 3 bear elliptic umbilics. The axes of order 4 bear degenerate umbilics of index $+1$ (case of the octahedron) or -1 (case of the cube). The axes of order 5 bear degenerate umbilics of index $+1$ (case of the dodecahedron and of the icosahedron). Moreover there are 12 hyperbolic umbilics of index $+1/2$ in some planes of symmetry in the case of the tetrahedron, and 24 in the case of the cube (see Table 1 of [17] for more details). It must also be noted that every D_4^- of each poly-astroid is surrounded by three symmetric butterflies, which are defined in [15, 16, 29]. Of course, for each polyhedron, the total index I of the umbilics is found to be equal to 2, i.e. the Euler characteristic of W .

To understand the generality of these results, let us apply the condition $I = 2$ simultaneously with the condition that the umbilics have an index i as small as possible ($|i| \leq 1$) and are compatible with the polyhedral symmetry. For instance, for the dodecahedral symmetry, one has to put elliptic umbilics on the 20 axes of order 3 (contribution $20(-1/2) = -10$ to I) and degenerate umbilics of index $+1$ on the 12 axes of order 5 (contribution $+12$ to I). This solution is obtained by starting from the dodecahedron

(Fig. 3d) or from the icosahedron. For the tetrahedral symmetry, the contribution of the 8 elliptic umbilics on the axes of symmetry 3 (contribution -4) has to be completed by the contribution of 12 additional hyperbolic umbilics of index $+1/2$ in 12 planes of symmetry (contribution $+6$). This solution is realized by our poly-astroid represented in Fig. 3a. It is also realized by the caustic of the “bumpy tetrahedron” of the reference [27]. The cubic case is surprising. There exists a simple solution with umbilics located only on the symmetry axes: 8 elliptic umbilics on the axes of order 3 (contribution -4) and 6 degenerate umbilics of index $+1$ on the axes of order 4 (contribution $+6$). This solution is obtained in our example by starting from the octahedron (Fig. 3c). However there exists another solution with the opposite index for the umbilics on the axes of order 4: 8 elliptic umbilics on the axes of order 3 (contribution -4), 6 degenerate umbilics of index -1 on the axes of order 4 (contribution -6), and 24 hyperbolic umbilics of index $+1/2$ on planes of symmetry (contribution $+12$). This solution is found in our example by starting from the cube (Fig. 3b). Other different poly-astroids exist, but they have a greater number of umbilics or higher indices (in absolute value). The four poly-astroids in Fig. 3 represent, in this sense, the four elementary polyhedral caustics.

The cubic astroid found in [32] corresponds to our octahedral case. Our results show that the index of its umbilics on the axes of symmetry of order 4 is equal to $+1$.

4. Conclusion. Caustics associated with biperiodically deflected rays and with stability diagrams of magnetic fine particle systems provide the first experimental examples of *compact* caustics. The topology of these compact caustics is constrained by the Chekanov formula. This *topological* constraint may be experimentally checked by determining the indices of the umbilics by numerical calculation of some elements (singular set, kernel of the Lagrangian projection, cusp lines and characteristics) in the phase space, or by direct observation in the physical space of the relative position of the rays with respect to the cusp lines passing through the umbilics. We find that biperiodic caustics, due to the deflection of the rays through a nematic liquid crystal layer, is the projection of a critical set having a non-zero Euler characteristic (-8).

Moreover, physical laws or boundary conditions may impose a global symmetry to the physical system. An additional *geometrical* constraint is then introduced: the different types of caustic points must be compatible with the symmetry. Interesting examples of this situation are provided by the caustics generated by surfaces with polyhedral symmetry. In that case, four elementary types of global configurations exist. Except for the tetrahedral symmetry, these caustics contain degenerate umbilics of integer index ± 1 .

References

- [1] V. I. Arnol'd, *Singularities of Caustics and Wave Fronts*, Math. Appl. (Soviet Ser.) 62, Kluwer Academic Publ., Dordrecht, 1990.
- [2] V. I. Arnol'd, *Normal forms of functions near degenerate critical points, the Weyl groups of A_k , D_k , E_k , and Lagrangian singularities* (in Russian), Funktsional. Anal. i Prilozhen. 6 (1972), no. 4, 3–25; English transl.: Funct. Anal. Appl. 6 (1972), 254–272.

- [3] V. I. Arnol'd, *Perestroikas of singularities of potential flows in collisionless media and metamorphoses of caustics in 3-space*, J. Soviet Math. 32 (1986), 229–257.
- [4] V. I. Arnol'd, V. V. Goryunov, O. V. Lyashko and V. A. Vasil'ev, *Singularity theory. II. Classification and applications*, in: Dynamical Systems VIII, Encyclopaedia Math. Sci. 39, Springer, Berlin, 1993, 1–235.
- [5] M. V. Berry, *Waves and Thom's theorem*, Adv. in Phys. 25 (1976), 1–26.
- [6] M. V. Berry and J. H. Hannay, *Umbilic points on Gaussian random surfaces*, J. Phys. A 10 (1977), 1809–1821.
- [7] M. V. Berry, J. F. Nye and F. J. Wright, *The elliptic umbilic diffraction catastrophe*, Philos. Trans. Roy. Soc. London Ser. A 291 (1979), 453–484.
- [8] M. V. Berry and C. Upstill, *Catastrophe optics: Morphologies of caustics and their diffraction patterns*, in: Progress in Optics, Vol. XVIII, E. Wolf (ed.), North-Holland, Amsterdam, 1980, 257–346.
- [9] M. Born and E. Wolf, *Principles of Optics*, Pergamon Press, Oxford, 1980.
- [10] A. Cayley, *On the centro-surface of an ellipsoid*, Trans. Cambridge Philos. Soc. 12 (1873), Part I, 319–365.
- [11] Yu. V. Chekanov, *Caustics in geometrical optics* (in Russian), Funktsional. Anal. i Prilozhen. 20 (1986), 66–69, 96; English transl.: Funct. Anal. Appl. 20 (1986), 223–226.
- [12] G. Darboux, *Sur la forme des lignes de courbure dans le voisinage d'un ombilic*, in: Leçons sur la théorie générale des surfaces, Vol. IV, Gauthier-Villars, Paris, 1896, 448–465.
- [13] P.-G. de Gennes and J. Prost, *The Physics of Liquid Crystals*, Clarendon Press, Oxford, 1993.
- [14] J. Guckenheimer, *Caustics and non-degenerate Hamiltonians*, Topology 13 (1974), 127–133.
- [15] S. Janeczko and M. Roberts, *Classification of symmetric caustic I: Symplectic equivalence*, in: Singularity Theory and its Applications, Part II, M. Roberts and I. Stewart (eds.), Lecture Notes in Math. 1463, Springer, Berlin, 1991, 193–219.
- [16] S. Janeczko and M. Roberts, *Classification of symmetric caustic II: Caustic equivalence*, J. London Math. Soc. (2) 48 (1993), 178–192.
- [17] A. Joets, M. Monastyrsky and R. Ribotta, *Ensembles of singularities generated by surfaces with polyhedral symmetry*, Phys. Rev. Lett. 81 (1998), 1547–1550.
- [18] A. Joets and R. Ribotta, *Hydrodynamic transitions to chaos in the convection of an anisotropic fluid*, J. Physique 47 (1986), 595–606.
- [19] A. Joets and R. Ribotta, *Structure of caustics studied using the global theory of singularities*, Europhys. Lett. 29 (1995), 593–598.
- [20] A. Joets and R. Ribotta, *A geometrical model for the propagation of rays in an anisotropic inhomogeneous medium*, Optics Communications 107 (1994), 200–204.
- [21] A. Joets and R. Ribotta, *Experimental determination of a topological invariant in a pattern of optical singularities*, Phys. Rev. Lett. 77 (1996), 1755–1758.
- [22] M. È. Kazarian, *Umbilical characteristic number of Lagrangian mappings of 3-dimensional pseudo-optical manifolds*, in: Singularities and Differential Equations, S. Janeczko, W. Zajączkowski and B. Ziemian (eds.), Banach Center Publ. 33, Warsaw, 1996, 161–170.
- [23] M. Kline and I. Kay, *Electromagnetic Theory and Geometrical Optics*, Interscience Publ., New York, 1965.
- [24] L. Landau et E. Lifchitz, *Électrodynamique des milieux continus*, Éditions Mir, Moscou, 1969.
- [25] J. F. Nye and J. H. Hannay, *The orientations and distortions of caustics in geometrical optics*, Optica Acta 31 (1984), 115–130.
- [26] D. Panov, private communication.

- [27] I. R. Porteous, *Geometric Differentiation for the Intelligence of Curves and Surfaces*, Cambridge Univ. Press, Cambridge, 1994.
- [28] R. Ribotta and A. Joets, *Pinching instability of convective rolls in an anisotropic fluid: first step to chaos*, J. Physique 47 (1986), 739–743.
- [29] M. Roberts and V. M. Zakalyukin, *Symmetric wavefronts, caustic and Coxeter groups*, in: Singularity Theory, D. T. Lê, K. Saito and B. Teissier (eds.), World Sci. Publ., River Edge, 1995, 594–626.
- [30] J. Sotomayor and C. Gutiérrez, *Structurally stable configurations of lines of principal curvature*, Astérisque 98–99 (1982), 195–215.
- [31] A. Thiaville, *Extensions of the geometric solution of the two-dimensional coherent magnetization rotation model*, J. Magn. Magn. Mater. 182 (1997), 5–18.
- [32] A. Thiaville, *Coherent rotation of magnetization in three dimensions: a geometrical approach*, to be published.
- [33] R. Thom, *Les singularités des applications différentiables*, Ann. Inst. Fourier (Grenoble) 6 (1956), 43–87.
- [34] R. Thom, *Sur la théorie des enveloppes*, J. Math. Pures Appl. (9) 41 (1962), 177–192.
- [35] R. Thom, *Topological models in biology*, Topology 8 (1969), 313–335.
- [36] V. M. Zakalyukin, *Reconstructions of fronts and caustics depending on a parameter and versality of mappings*, J. Soviet Math. 27 (1984), 2713–2735.
- [37] Ya. B. Zeldovich, *The desintegration of homogeneous matter into parts under the action of gravity*, Astrofizika 6 (1970), 319–335.